

SHEAR STRESS EFFECTS ON SCHLEMM'S CANAL CELLS

By

Nicole Ashpole

---

A Thesis Submitted to the Faculty of the

BIOMEDICAL ENGINEERING PROGRAM

In Partial Fulfillment of the Requirements

For the Degree of

MASTER OF SCIENCE

In the Graduate College

THE UNIVERSITY OF ARIZONA

2012

## STATEMENT BY AUTHOR

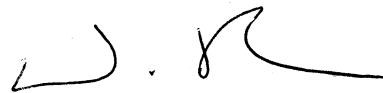
This thesis has been submitted in partial fulfillment of requirements for an advanced degree at The University of Arizona and is deposited in the University Library to be made available to borrowers under rules of the Library.

Brief quotations from this thesis are allowable without special permission, provided that accurate acknowledgement of source is made. Requests for permission for extended quotation from or reproduction of this manuscript in whole or in part may be granted by the head of the major department or the Dean of the Graduate College when in his or her judgment the proposed use of the material is in the interests of scholarship. In all other instances, however, permission must be obtained from the author.

SIGNED: Nicole E Ashpole

## APPROVAL BY THESIS DIRECTOR

This thesis has been approved on the date shown below:



Dr. W. Daniel Stamer

6/7/12

Date

## ACKNOWLEDGEMENTS

I first wish to thank my committee for their support and guidance in the creation of this thesis.

Their generosity is much appreciated as I move on to the next stage of my career.

W. Daniel Stamer, Ph.D.

Jonathan VandeGeest, Ph.D.

Ronald Lynch, Ph.D.

Jim Schwiegerling, Ph.D.

Second I wish to acknowledge the financial support of the Research to Prevent Blindness and National Institutes of Health (Grant #EY017007 and #EY022359).

Third I would like to acknowledge and thank Kristen Perkumas and Emely Hoffman for their assistance in teaching me many of the techniques used in this thesis, such as cell culture and Western blots.

I wish to dedicate this thesis to my parents,  
my siblings and my fiancé for their encouragement  
and support throughout my academic career.

## TABLE OF CONTENTS

STATEMENT BY AUTHOR .....	2
ACKNOWLEDGEMENTS .....	3
DEDICATION .....	4
LIST OF TABLES .....	7
LIST OF ILLUSTRATIONS .....	8
ABSTRACT .....	9
1 INTRODUCTION .....	10
2 BACKGROUND .....	12
2.0 The Eye and the Conventional Outflow Pathway .....	12
2.1 Sclemm’s canal .....	12
2.2 Nitric Oxide .....	13
2.3 Production of Nitric Oxide .....	15
3 MATERIALS AND METHODS.....	18
3.0 Shear Stress Experiments .....	18
3.0.0 HUVECS and SC Cell Culture .....	18
3.0.1 $\mu$ -Slide Preparation.....	18
3.0.2 Ibidi Pump System Preparation .....	19
3.1 Nitric Oxide Detection .....	24
3.1.0 NO Probe .....	24
3.1.1 DAF-FM Diacetate Fluorescence .....	27
4 RESULTS.....	29
4.0 Phase contrast Microscopy .....	29
4.1 Nitric Oxide Probe Analysis .....	30
4.1.0 Comparison of two NO detection Methods .....	30
4.2 DAF-FM Fluorescence Analysis.....	33
4.2.0 HUVECS and SC DAF-FM Figures .....	33
4.2.1 Quantification of NO Fluorescence .....	35
5 DISCUSSION .....	36
5.0 Cell Alignment .....	36

5.1	Expression of Nitric Oxide .....	36
5.1.0	NO Probe .....	36
5.1.1	DAF-FM Diacetate Fluorescence .....	38
6	FUTURE WORK.....	40
7	CONCLUSIONS .....	43
	APPENDIX .....	44
	Shear Stress on Schlemm's Canal <sup>7</sup> .....	44
	Ibidi Pump Shear Stress Calculations .....	46
	References.....	48

## LIST OF TABLES

Table 1: Yellow-Green Perfusion Set Specifications <sup>33</sup> .....	20
--	----

## LIST OF ILLUSTRATIONS

Figure 1: Model of NO regulation of outflow .....	17
Figure 2: Perfusion Set-up (a) Sterile air filters (0.2 $\mu\text{m}$ , Teflon), (b) Syringe reservoirs, (c) Silicone tubing, (d) Branched tubes for insertion in pinch valves of fluidic unit, (e) Luer adapters to $\mu$ -slide, (f) Middle connector for set-up without the $\mu$ -slide <sup>33</sup> .....	20
Figure 3: Fluidic Unit Set-up <sup>33</sup> .....	21
Figure 4: Ibidi Pump Set-Up <sup>33</sup> .....	22
Figure 5: Positive Pressure Ibidi Pump System Set-up <sup>33</sup> .....	23
Figure 6: Calibration Curve obtained from NO Sensor with iNOII software plotting the current the sensor receives versus the time .....	25
Figure 7: Calibration Curve plotting Current versus the NO concentration.....	25
Figure 8: Locations where NO probe were placed (1) through the top of the reservoir (in between the filter and the black rubber and into the media in the reservoir (2) into a Y-connector that joins the perfusion set Luer connector and the $\mu$ -slide .....	27
Figure 9: Cell Alignment in HUVECS (Panel A and B) and SC cells (Panel C and D) at 0.1 dynes/cm <sup>2</sup> and 10.0 dynes/cm <sup>2</sup> , respectively .....	29
Figure 10: Calibration Curve for NO probe set-up 1 and 2. Probe 1 was used for the first set-up in which the NO probe was placed in the reservoir. Probe 2 was the NO probe used in the second set-up, in which the NO probe was connected to the system via a Y-connector.....	30
Figure 11: Comparing the response of the NO probe when probe is arranged in the First Set-Up (blue line) and in the Second Set-Up (red line). This figure shows the first 333 minutes of the experiment. The second set-up shows a relative increase in current around 70 minutes .....	31
Figure 12: NO probe readings from 333 minutes to 666 minutes. The current is beginning to decrease. ....	31
Figure 13: NO probe readings from 666 minutes to 1000 minutes .....	32
Figure 14: NO probe readings from 1000 minutes to 1333 minutes .....	32
Figure 15: NO probe readings from 1333 minutes to 1666 minutes .....	32
Figure 16: Nitric Oxide Production in HUVECS and Schlemm's Canal Cells. Panel A and E: 50 $\mu\text{M}$ DAF-FM probe treatment of Huvecs and Schlemm's Canal (SC) Cells, respectively, exposed to 0.1 dynes/cm <sup>2</sup> shear. Huvecs were exposed for 24 hours and SC cells were exposed for 1 week. <i>Panel B and F:</i> Huvecs and SC cells exposed to 10.0 dynes/cm <sup>2</sup> . <i>Panel C and G:</i> Positive Control – Huvecs and SC Cells exposed to 10.0 dynes/cm <sup>2</sup> with 100 $\mu\text{M}$ of NO Donor (L-Arginine) supplemented media. <i>Panel D and H:</i> Negative Control – Huvecs and SC Cells exposed to 10.0 dynes/cm <sup>2</sup> with 100 $\mu\text{M}$ eNOS inhibitor (L-Name) supplemented media. ....	34
Figure 17: Relative Fluorescence of HUVECS and SC Cells exposed to different conditions (n=5). .....	35
Figure 18: Desensitized NO probe reading at $\sim 360,000$ pA .....	38
Figure 19: Schematic of Flow through a Rectangular Cross Section <sup>46</sup> .....	47



## **ABSTRACT**

Nitric Oxide (NO) is a radical produced by endothelial NO synthase (eNOS), which is regulated by shear stress in vascular endothelia. In humans, shear stress levels in Schlemm's Canal (SC) are calculated to be comparable to that of arteries, particularly at elevated intraocular pressure (IOP), a risk factor for glaucoma. To test if NO is part of an IOP regulatory loop, we investigated the relationship between NO and shear stress in SC cells. Cells were seeded into Ibidi flow chambers and assayed for effects of continuous shear on cell alignment and NO production. Human umbilical vascular endothelial cells (HUVECS) were used as a positive control. Like HUVECS, SC cells aligned with the direction of flow. NO synthesis in both cell types doubled with an increase in shear from 0.1 to 10.0 dynes/cm<sup>2</sup>, suggesting that shear regulates NO production in SC cells and consequently may play a role in IOP regulation.

## 1 INTRODUCTION

Glaucoma is the second leading cause of blindness in the world, according to the World Health Organization <sup>1</sup>. In the United States alone, it is estimated that over 2.5 million people have glaucoma, and over 120,000 are blind because of glaucoma <sup>1</sup>. This accounts for approximately 9% to 12% of all cases of blindness <sup>1</sup>. Glaucoma refers to a family of eye diseases in which damage to the optic nerve results in permanent loss of vision. Types of glaucoma include primary open-angle glaucoma, normal-tension glaucoma, closed-angle glaucoma, congenital glaucoma and secondary glaucoma.

Primary open-angle glaucoma (POAG) is by far the most common form of glaucoma, accounting for more than 75% of total. This form of glaucoma occurs when aqueous humor drainage through the conventional outflow pathway (consisting of the Trabecular Meshwork and Schlemm's canal) is impaired at the molecular/cellular level and not simply via obstruction, although the mechanism is still unknown <sup>2,3</sup>. Resistance to drainage of aqueous humor results in an increase in intraocular pressure (IOP), which in turn often results in damage to optic nerve fibers at the level of the lamina cribrosa region of the optic nerve. A patient will usually not notice any changes in their vision in the beginning stages of POAG. However, as more and more ganglion cell fibers are lost over time a patient will notice blind spots (scotomas), typically in the periphery of their vision. As more of the nerve fibers die, these spots become larger until blindness results across the entire visual field.

Glaucoma can affect anyone of any age, ethnic race or gender. The elderly and Africans, however, are at a higher risk <sup>1</sup>. Currently glaucoma has no cure, and once vision is lost, it cannot be regained. Medication (such as timolol or latanoprost <sup>4</sup>) and/or surgery are targeted at

lowering IOP and have been shown effective at halting or slowing further vision loss<sup>5</sup>. IOP can be lowered by inhibiting the secretion of aqueous humor into the eye or by enhancing aqueous humor drainage from the eye. Unfortunately, approximately 10% of people with glaucoma and who receive proper medical treatment still experience blindness<sup>1</sup>; and far more continue to slowly lose vision because their IOP cannot be lowered enough.

## 2 BACKGROUND

### 2.0 The Eye and the Conventional Outflow Pathway

In the eye, a clear, colorless, fluid called aqueous humor is secreted into the eye via the ciliary epithelium in the posterior chamber of the eye, between the iris root and pars plana, the edge of the retina<sup>6</sup>. The aqueous humor flows through the pupil and into the anterior portion of the eye and nourishes the avascular tissues of the eye (lens, cornea and trabecular meshwork) before draining out of the eye<sup>7</sup>.

There are two pathways in which aqueous humor is drained from the eye: the primary outflow pathway, or the conventional outflow pathway, which is responsible for up to 90% of the aqueous humor drainage<sup>8</sup>; and the secondary pathway, the uveoscleral pathway. The conventional pathway consists of the trabecular meshwork and Schlemm's Canal, a circular vessel that is located between the cornea and ciliary muscle. The conventional outflow pathway is pressure sensitive, and resistance to aqueous humor outflow is generated deep into the conventional outflow pathway, where the TM and inner wall of SC interact<sup>6,9</sup>. Despite this route being the main path for aqueous humor outflow and the site of diseased tissue responsible for elevated IOP in glaucoma, there are currently no effective medical treatments that target the conventional pathway to improve eye facility.

### 2.1 Schlemm's canal

Schlemm's Canal is the first venous vessel that aqueous humor enters as it leaves the eye. The canal is made up of a monolayer of vascular-derived endothelial cells<sup>7,10,11</sup> and functions by collecting the aqueous humor from the anterior chamber of the eye and then delivering it into the systemic circulation via the anterior ciliary veins.

The endothelial lining of Schlemm's Canal can be divided into an "inner" and "outer" wall. The "inner" wall is a layer of endothelia that sits on a discontinuous basal lamina and is exposed to a basal to apical pressure gradient resulting in distension. The "outer" wall is a layer of endothelia that sits on a continuous basal lamina situated atop sclera, similar to other endothelia<sup>7</sup>. SC cells generally align in the direction of the length of the canal, turning in the direction of collector channels<sup>7</sup>. Shear through the canal, however, is a likely modulator for this cell alignment<sup>7</sup>.

It has been experimentally indicated that the Trabecular Meshwork and/or the inner wall of Schlemm's Canal are the primary sites of outflow resistance in a normal human eye<sup>6</sup>.

Intraocular pressure (IOP) is dependent on the episcleral venous pressure (inside SC),  $P_v$ ; the resistance generated by TM and SC cells,  $R$ ; uveoscleral flow,  $F_u$ ; and the rate of aqueous humor formation,  $F_{aq}$ <sup>6</sup>:

$$IOP = P_v + (F_{aq} - F_u) * R \quad \text{(Equation 1)}$$

Previous work has derived the relationship between IOP and the shear on Schlemm's Canal cells (see Appendix – Shear Stress on Schlemm's Canal)<sup>7</sup>. When the IOP is high and the Schlemm's Canal has a small diameter, shear stress levels have been calculated to increase in Schlemm's Canal<sup>7</sup>. Interestingly, these calculated shear levels are comparable to the shear values that large coronary arteries receive (namely 2-20 dynes/cm<sup>2</sup>)<sup>127</sup>. A key signaling molecule under conditions of high shear in endothelial cells is Nitric Oxide.

## 2.2 Nitric Oxide

Nitric Oxide (NO) is a free radical that is generated by the conversion of L-Arginine to L-Citrulline by one of three NO synthases (NOS): nNOS (found primarily in neuronal tissues, but also in skeletal muscles), iNOS (found primarily in immune-activated macrophage cell lines, but also

cardiac myocytes and vascular smooth muscle cells) and eNOS (found primarily in endothelial cells, but also in myocytes and blood platelets)<sup>4, 13</sup>.

NO, once produced, performs functions through the activation of soluble guanylyl cyclase (sGC) enzyme which results in the formation of cyclic GMP (cGMP)<sup>14</sup>, or by the modulation of transcription<sup>15</sup>. NO is a gas that is soluble in tissues and freely diffusible across cell membranes. It functions intracellularly as a second messenger that responds to plasma membrane receptor activation, and extracellularly as a paracrine factor that relays information between various cells<sup>16</sup>. NO, therefore, has a plethora of functions including decreasing platelet aggregation and neutrophil adhesion<sup>17</sup>; regulating the assembly and disassembly of intercellular junctions which affects endothelial permeability<sup>18</sup>; and muscle relaxation, resulting in vasodilation<sup>15</sup>. Because of its function, abnormal NO concentrations have been implicated in several diseases, such as hypertension, heart failure and hypercholesterolemia<sup>19</sup>.

Interestingly, NO deficiency has been related to several eye diseases, including glaucoma<sup>16, 20</sup>. In particular, abnormalities in NO production appear with higher frequency in patients with primary open-angle glaucoma. To support this, several NO donating compounds have been found to increase conventional outflow facility and decrease IOP in transgenic mice, rabbits, pigs, dogs, monkeys and humans<sup>4, 6, 8, 9, 20, 21</sup>. In contrast, perfusion of human eyes with NOS inhibitors resulted in a decrease in the facility of outflow<sup>22</sup>. Even direct topical or intracameral application of NO agonists, have likewise been reported to alter outflow facility<sup>23-25</sup>.

Comparing the ciliary muscle and the outflow pathway between anterior segments of healthy individuals and anterior segments of individuals with a history of POAG, it was found that the anterior longitudinal ciliary muscle, the TM and the SC showed a marked reduction of NO

production in POAG individuals as indicated by NADPH-diaphorase, an NO-indicator marker<sup>24</sup>.

This suggests that NO production is somehow impaired in POAG individuals.

Both cell types in the human conventional outflow pathway (the SC and the TM), along with the ciliary muscle, have been shown to generate NO by using a variety of indicators. This includes the NO indicator marker, NADPH-diaphorase, a direct biochemical assay and immunocytochemical localization of NO synthase isoforms<sup>26</sup>. This study found that primarily eNOS was present in these postmortem human eyes<sup>26</sup>.

### **2.3 Production of Nitric Oxide**

The three NOS enzymes are NADPH, calcium/calmodulin-dependent enzymes<sup>27</sup>. Several ocular components, such as the trabecular meshwork and Schlemm's canal, have been shown to express constitutive NOS<sup>26</sup>; although there is some debate on whether the endothelial NOS (eNOS) or the inducible NOS (iNOS) is the main NOS enzyme implicated in the maintenance of vascular tone and for NO generation<sup>22,26</sup>. Rats, after all, have been demonstrated to express a little iNOS activity in the cranial ganglia and the choroid, the vascular layer of the eye<sup>28</sup>. It has been shown, however, that there is an enrichment of eNOS in the human outflow system and in the ciliary muscle<sup>26</sup>. Interestingly, a variant in the promoter region of the eNOS gene was seen in a number of patients with familial POAG<sup>27</sup>, suggesting another link between eNOS and glaucoma. Therefore, eNOS is the most likely regulator of NO production within the outflow pathway and thus may be an important factor in the regulation of IOP, which if impaired can lead to glaucoma.

As eNOS may be an important regulator of IOP, it is important to understand what regulates this enzyme's activity. eNOS activity and abundance has been shown to be regulated by shear stress

in vascular endothelia both in flow chambers with controlled shear stress conditions in vitro and in transgenic mice in vivo<sup>29-31</sup>. This indicates that an increase in shear can lead to the up-regulation in eNOS and consequently an increase in the concentration of NO. The release of NO then results in an increase in outflow facility which reduces the IOP, consequently decreasing the shear being applied to the conventional outflow pathway.

Because of this potential role of shear on regulating IOP, we investigated the relationship between Nitric Oxide and eNOS production, and shear stress in cultured human SC cells. Our central hypothesis is that shear stress in Schlemm's Canal functions as a modulator within an endogenous feedback loop. This loop detects the changes in IOP through effects on shear stress in SC as the canal lumen diameter decreases, in part, through NO signaling (Figure 1). For this work, we hypothesized that shear leads to an increase in eNOS and NO production in Schlemm's Canal cells, similarly to other endothelial cells.



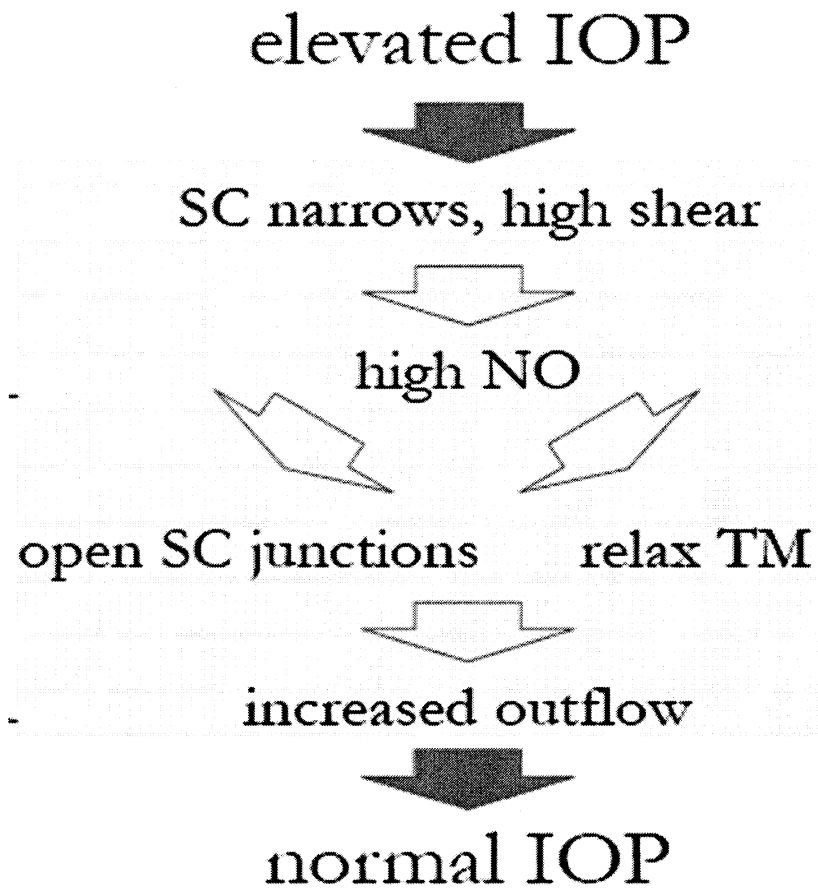


Figure 1: Model of NO regulation of outflow

## 3 MATERIALS AND METHODS

### 3.0 Shear Stress Experiments

Shear Stress was applied to confluent cells with the use of an ibidi pump system which is capable of maintaining defined shear stress level across a surface of cells. SC cells were exposed to various shear levels for a set amount of time. The cells were then analyzed for NO production and eNOS expression. HUVECS were used as a positive control. Other controls include exposing the cells to shear with media supplemented with an NO donor (100  $\mu$ M L-Arginine) and an eNOS inhibitor (100  $\mu$ M L-Name).

#### 3.0.0 HUVECS and SC Cell Culture

The cells used in these experiments were HUVECS and SC cells. The medium used for HUVECS was Medium 199 (Gibco by Life Technologies, Grand Island, NY) supplemented with 15% Hyclone Fetal Bovine Serum or FBS (Thermo Scientific, South Logan, Utah), Penicillin Streptomycin Glutamine or PSG (100 U/mL, Gibco by Life Technologies, Grand Island, NY), heparin sodium salt (90  $\mu$ g/mL, Sigma-Alrich, St. Louis, Mo) and Endothelial Mitogen (0.1 mg/mL, Biomedical Technology, Inc, Stoughton, Ma). The medium used for SC cells was DMEM Low Glucose 1X Medium (Gibco by Life Technologies, Grand Island, NY) supplemented with 15% FBS and PSG (100 U/mL). The other mediums used for experiments included both media's supplemented with 100  $\mu$ M L-Arginine cell-culture tested (Sigma, St. Louis, Mo) and 100  $\mu$ M N<sub>w</sub>-Nitro-L-arginine methyl ester chloride or L-Name (Sigma, St. Louis, Mo).

#### 3.0.1 $\mu$ -Slide Preparation

Cells were loaded onto  $\mu$ -slides I<sup>0.6</sup> (ibidi, Munich, Germany) and allowed to set in an incubator at 37°C with 5.0% CO<sub>2</sub>. Slides were provided with an ibiTreat surface, a physical modification used to improve cell adhesion on the  $\mu$ -slide<sup>32</sup>. This surface is comparable to standard cell

culture flasks and Petri dishes<sup>32</sup>. These  $\mu$ -slides are capable of holding 150  $\mu$ L in volume. They are 600  $\mu$ m in height and an area of 2.5 cm<sup>2</sup>.

HUVECS were loaded onto  $\mu$ -slides and allowed to settle for at least one to three days before being hooked up to the Ibidi pump system for shear stress experiments. Schlemm's Canal 60.4 cells were loaded onto  $\mu$ -slides and allowed to settle for at least two before shear was applied.

### **3.0.2 Ibidi Pump System Preparation**

The Ibidi Pump System (ibidi, Munich, Germany) was set-up as per protocol<sup>33</sup>. In a hood, the yellow/green type perfusion set (Shown in Figure 2, Specifications shown in Table 1) was attached to reservoirs and the reservoirs were placed into the holders on the fluidic unit (Figure 3). A spare  $\mu$ -slide, containing no cells, was connected to the perfusion set. The perfusion set and the reservoirs were rinsed in 70% ethanol three times, and then rinsed in Dulbecco's Phosphate Buffered Saline 1x (DPBS) without Calcium Chloride or Magnesium Chloride (Gibco by Life Technologies, Grand Island, NY) three times, before being filled with medium. The branched tubes of the perfusion set were then set in the designated slots of the fluidic unit. Sterile Sartorius Minisart filters (0.2  $\mu$ m pore size, Teflon, Sigma-Aldrich, St. Louis, Mo) were placed on top of the reservoirs and connected to the top air pressure tubes of the fluidic unit.

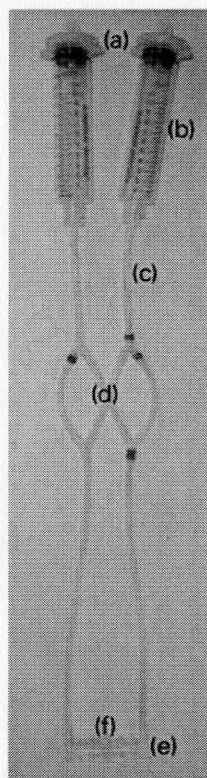


Figure 2: Perfusion Set-up (a) Sterile air filters (0.2  $\mu\text{m}$ , Teflon), (b) Syringe reservoirs, (c) Silicone tubing, (d) Branched tubes for insertion in pinch valves of fluidic unit, (e) Luer adapters to  $\mu$ -slide, (f) Middle connector for set-up without the  $\mu$ -slide<sup>33</sup>

Table 1: Yellow-Green Perfusion Set Specifications<sup>33</sup>

Perfusion Set yellow/green (#10964)							
		Inner diameter: 1.6 mm			Tube length: 50 cm		
		Total working volume: 13.6 ml			Dead volume of tubing: 2.8 ml		
	Growth area [ $\text{cm}^2$ ]	Channel volume [ $\mu\text{l}$ ]	Flow rate [ml/min]		Shear stress [ $\text{dyn}/\text{cm}^2$ ]		
			MIN	MAX	MIN	MAX	
$\mu$ -Slide I 0.2 Luer	2.5	50	1.03	17.00	5.28	87.20	
$\mu$ -Slide I 0.4 Luer	2.5	100	1.91	25.95	2.51	34.16	
$\mu$ -Slide I 0.6 Luer	2.5	150	1.98	27.44	1.19	16.49	
$\mu$ -Slide I 0.8 Luer	2.5	200	2.13	30.25	0.47	10.51	
$\mu$ -Slide VI 0.4	0.6	30	2.06	28.95	3.63	51.00	
$\mu$ -Slide $\gamma$ -shaped	2.8	110	1.94	26.60	4.41	60.50	
without slide	-	(75)	2.44	36.02	-	-	

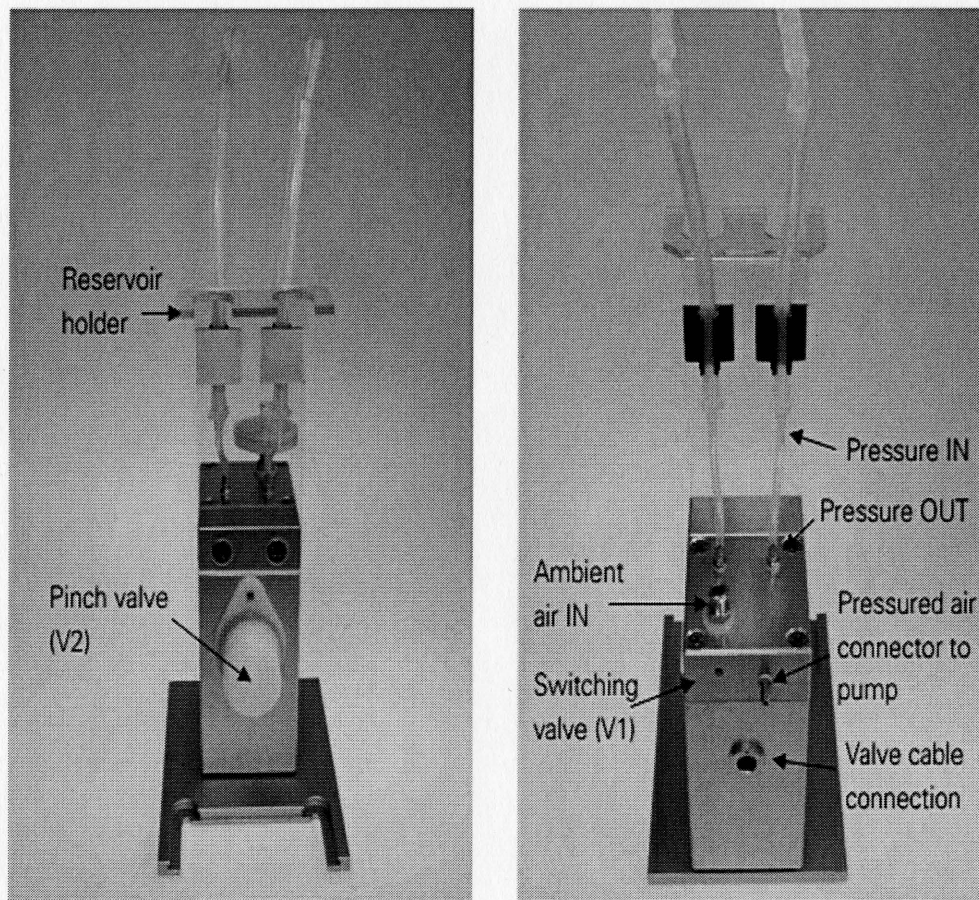


Figure 3: Fluidic Unit Set-up<sup>33</sup>

The fluidic unit was then connected to the pump via electric cable to control the switching of the valves; and to the front air port directly on the pump (Figure 4) via silicone tubing to achieve positive pressure. The fluidic unit was then placed into an incubator at 37°C and 5.0% CO<sub>2</sub>. The rear air port was connected to a silica drying bottle via silicone tubing and the silica bottle, in turn, had a tube running into the incubator so that the air being pumped into the system was kept at 37°C, with 5.0% CO<sub>2</sub> and filtered of any pathogens to maintain sterility in the system.

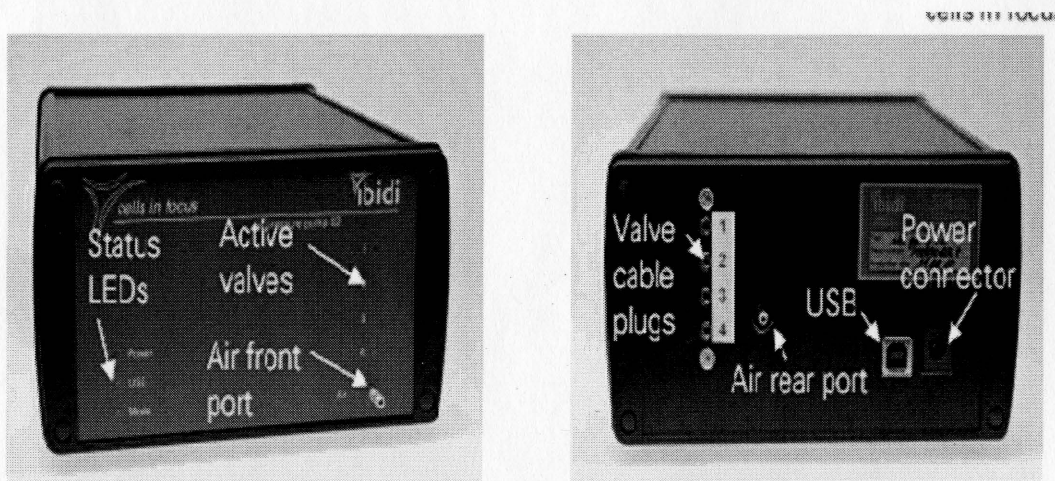


Figure 4: Ibidi Pump Set-Up <sup>33</sup>

An automated cycle was run using the PumpControl software to remove the bubbles. The software ran a shear of  $10.0 \text{ dynes/cm}^2$  across the blank  $\mu$ -slide for a minimum of 30 minutes. The media was left to warm for a minimum of two hours before the system was calibrated. Calibration, as per the manual <sup>33</sup>, was performed by setting the program to run at  $10.0 \text{ dynes/cm}^2$ . Then the reservoirs were observed to view how much the level of media changed with respect to time to find the flow rate,  $\phi$  (mL/min). Putting the flow rate into the program allowed for the program to adjust the calibration setting which in turn adjusted the air pressure being applied to the system.

Once the cells in the  $\mu$ -slides reached confluence, the  $\mu$ -slides were attached to the Ibidi Pump System in a hood (final set-up shown in Figure 5). Positive pressure was applied to the cells at various shear rates.

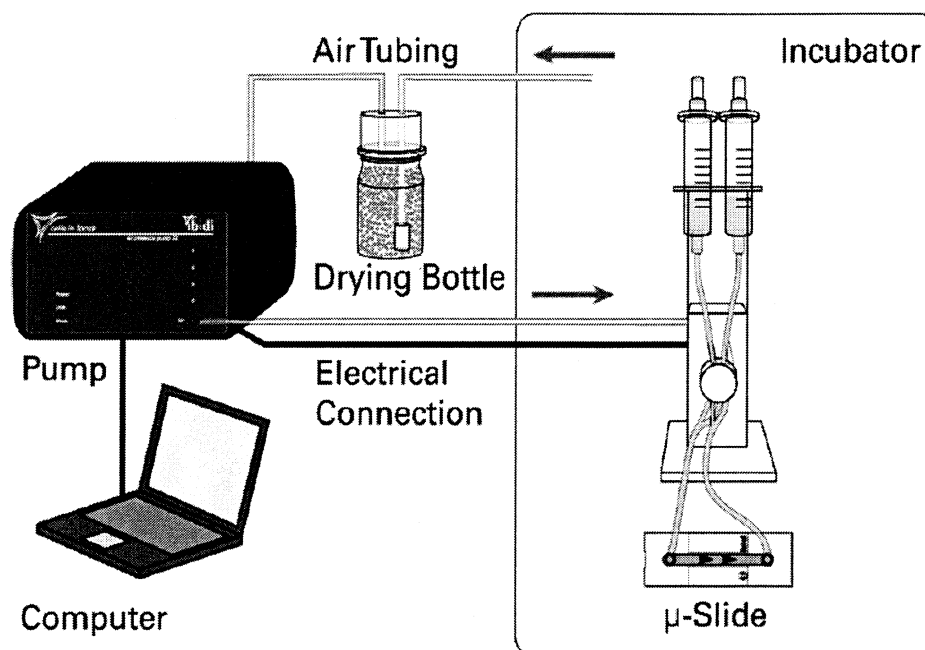


Figure 5: Positive Pressure Ibidi Pump System Set-up<sup>33</sup>

The shears applied to the HUVEC  $\mu$ -slides were 0.1 and 10.0 dynes/cm<sup>2</sup> (see Appendix – Ibidi Pump Shear Stress Calculations) for 24 hours when cell alignment could be confirmed with phase contrast microscopy (Olympus IX70 Microscope and Olympus U-PMTVC Camera, Olympus America Inc, Center Valley, Pa). The shears applied to SC cell  $\mu$ -slides were also 0.1 and 10.0 dynes/cm<sup>2</sup>, however shear was applied for a minimum of 1 week before cell alignment could be confirmed with phase contrast microscopy. Both cell types were exposed to 10.0 dynes/cm<sup>2</sup> with both the 100  $\mu$ M L-Arginine supplemented media and 100  $\mu$ M L-Name supplemented media.

As per protocol given by the company<sup>34</sup>, when the shear exceeded 2.00 dynes/cm<sup>2</sup> the cells needed to be adapted to low levels of shear, before being exposed to higher levels of shear. Therefore, the shear experiments for 10.0 dynes/cm<sup>2</sup> began with the cells being exposed to 30 minutes of 2.00 dynes/cm<sup>2</sup>, before increasing to 5.00 dynes/cm<sup>2</sup> also for 30 minutes. After this

shear-conditioning section, the shear was increased to 10.0 dynes/cm<sup>2</sup> for 24 hours for HUVECS and 1 week for SC cells.

### **3.1 Nitric Oxide Detection**

#### **3.1.0 NO Probe**

Originally, in order to detect Nitric Oxide, a NO probe was used: inNO-T-II NO measuring system along with an amiNO-700 model NO sensor and inoll software (Innovative Instruments, Inc, Tampa, FL) borrowed from Dr Nicholas Delamere of the Department of Physiology at the University of Arizona.

Before use, the NO probe needed to be calibrated through a protocol provided by the company. The sensor is first submerged in milliQ water for a minimum of 3-4 hours or overnight to polarize the probe. Then the probe is placed in a calibration solution of 18.0 mL of milliQ water and 2.0 mL of 1.0 M sulfuric acid and the probe is connected to the meter. A magnetic stir bar is used to keep the solution mixing. The sensor is fixed in place with a clamp. Once the sensor is reading a stable background current, the sensor is zeroed.

Then 10.0  $\mu$ L of 100  $\mu$ M NaNO<sub>2</sub> solution (Sodium Nitrite from Acros Organic in Thermo Fisher Scientific, NJ) is added to the calibration solution resulting in a 50 nM NO solution. The sensor records the current in pA (Figure 6) that correlates to this concentration. Once the sensor reaches its peak and begins to decrease, 20  $\mu$ L of the 100  $\mu$ M NaNO<sub>2</sub> solution is added for a final concentration of 100 nM NO. This peak is recorded and finally 40  $\mu$ L of 100  $\mu$ M NaNO<sub>2</sub> solution is added for a concentration of 200 nM.



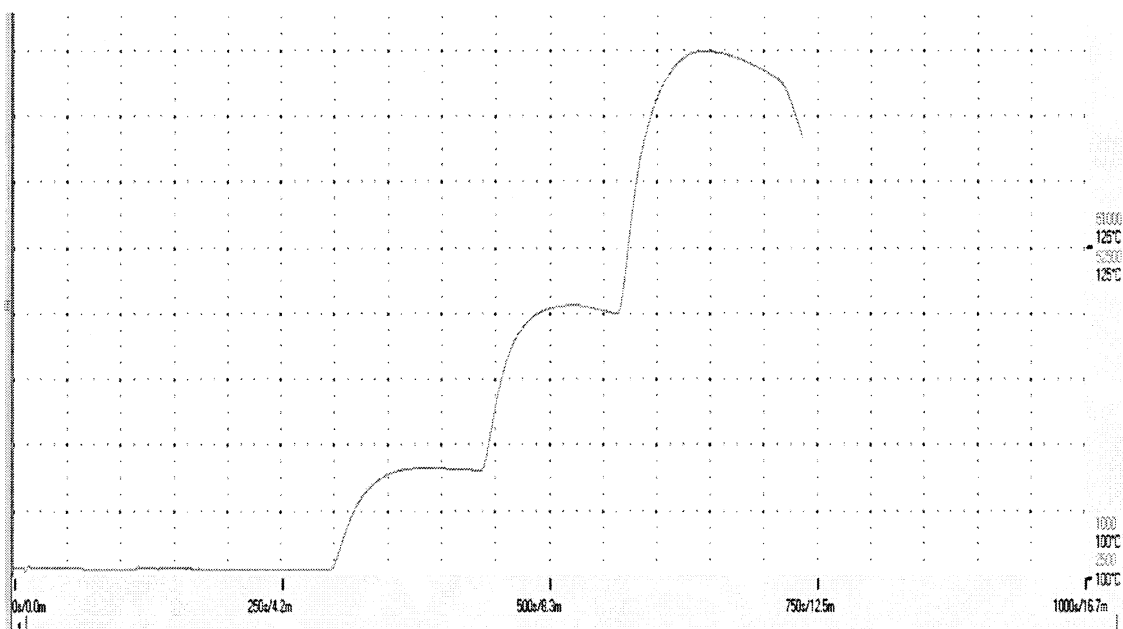


Figure 6: Calibration Curve obtained from NO Sensor with iNOII software plotting the current the sensor receives versus the time

The Calibration equation is then obtained by plotting the current found by the software versus the concentration of Nitric Oxide. Microsoft Excel is then used to find the equation.

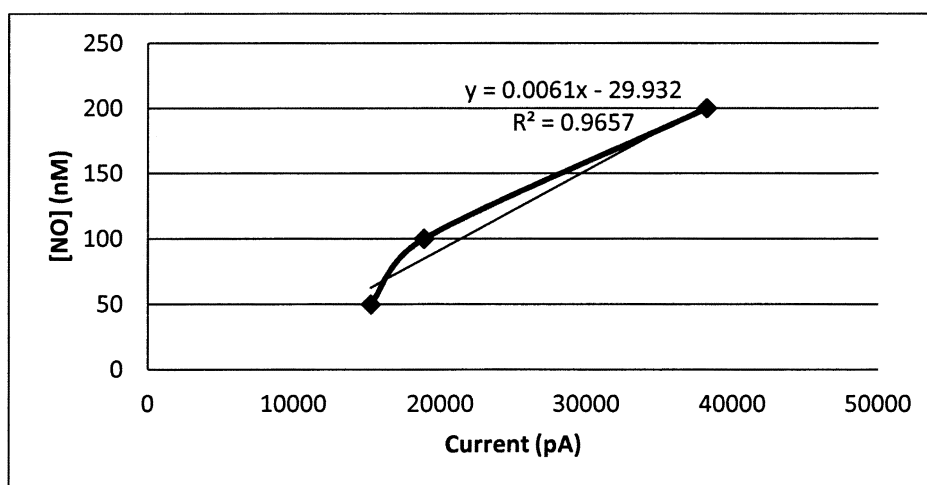
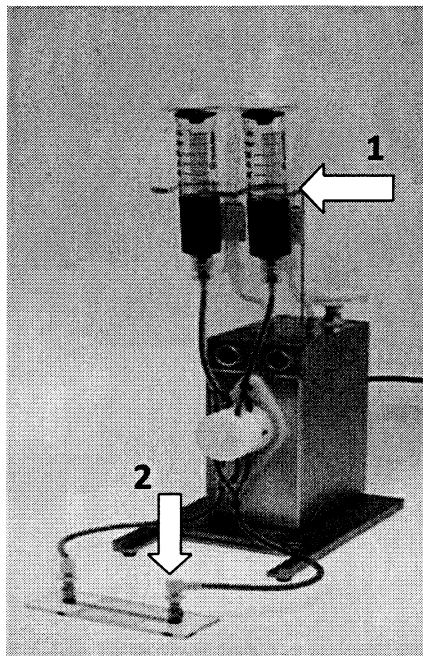


Figure 7: Calibration Curve plotting Current versus the NO concentration

The probe was placed in two locations within the ibidi Pump System in order to determine where the NO probe was most effective at reading the concentrations of NO while the cells were being exposed to shear rates. The first set-up involved the probe being set in the reservoir (Figure 8) and the second set-up involved setting the probe in a Luer Y-connector that was located in between the  $\mu$ -slide and the perfusion set Luer connector (Figure 8). The probe was locked in place in the first set-up by being poked through the rubber fitting that holds the filter in place and keeps the system enclosed. To keep the filter attached to the reservoir, parafilm was wrapped around in order to ensure the filter did not detach from the reservoir in the course of the experiment.

The probe is locked in place in the second set-up with a Luer lock cap with a hole to allow for the probe to fit through. Super glue and parafilm are used to fill in the gap between the Luer cap and the probe. The cap was then screwed onto the Y-connector allowing the sensor to be exposed to the media. In both conditions, the probes were exposed to the media overnight such that the probes stabilized. The NO program was started for approximately 10-15 minutes to show the baseline that the probe had reached, in the morning of the following day. Then the shear stress experiments were then started.



**Figure 8:** Locations where NO probe were placed (1) through the top of the reservoir (in between the filter and the black rubber and into the media in the reservoir (2) into a Y-connector that joins the perfusion set Luer connector and the  $\mu$ -slide

### 3.1.1 DAF-FM Diacetate Fluorescence

A secondary Nitric Oxide Probe used was a DAF-FM Diacetate (4-Amino-5-Methylamino-2',7'-Difluorofluorescein Diacetate) probe (Life Technologies, Grand Island, NY). DAF-FM is a reagent that is used to detect and quantify low concentrations of NO and is essentially non-fluorescent until it reacts with NO to form benzotriazole, which is fluorescent. DAF-FM is excited by  $\sim 495$  nm light and emits at 515 nm.

A 5 mM stock solution of the DAF-FM diacetate (Molecular Weight = 496) was made with 0.4 mL high-quality anhydrous DMSO.

As per the protocol provided by Life Technologies<sup>35</sup>, once the cells prepared on the  $\mu$ -slide and exposed to shear with the ibidi Pump System, the  $\mu$ -slide was incubated with 50  $\mu$ M of the DAF-FM diacetate for 45 minutes at 37°C. The cells were then washed with Dulbecco's Phosphate

Buffered Saline 1x (DPBS) without Calcium Chloride or Magnesium Chloride (Gibco by Life Technologies, Grand Island, NY) to remove the excess probe and replaced with fresh medium. The cells were then incubated at 37°C for an additional 15 minutes.

The fluorescence was imaged with a Nikon Eclipse TE2000-U Microscope (Nikon Instruments Inc, Melville, NY) attached to a Cooke SensiCam High Performance (Motion Engineering Company, Inc, Indianapolis, In). This equipment belongs to Dr. Pak Wong, Aerospace and Mechanical Engineering Department at the University of Arizona. Images were taken at 10x magnification with a  $\infty$  PH filter and a green light filter.

Several pictures were taken across the entire  $\mu$ -slide for a minimum of five final images per cell type per shear stress condition. Images were analyzed using Image J software with the Nikon microscope and SensiCam specific plug-in at 10x magnification. For each image the mean fluorescence of cells located throughout the picture was measured at 15 different points. These 15 values were then averaged to get an overall fluorescence value. The same was done for 5 different points of the background, the non-fluorescent portion of the figures located between cells. The background fluorescence average was then subtracted from the cell fluorescence average to get the relative fluorescence of the cells. All points measured for fluorescence was taken at random.

## 4 RESULTS

### 4.0 Phase contrast Microscopy

Alignment of cells exposed to shear was assessed with phase contrast microscopy. HUVEC  $\mu$ -slides were exposed to 0.1 dynes/cm<sup>2</sup> (Figure 9, Panel A) and 10.0 dynes/cm<sup>2</sup> (Figure 9, Panel B) for 24 hours. Exposure to 0.1 dynes/cm<sup>2</sup> did not result in cell alignment, however, exposure to 10.0 dynes/cm<sup>2</sup> did result in full alignment at the end of 24 hours.

Similarly, we found that exposing SC 60.4 cells for 1 week, at 0.1 dynes/cm<sup>2</sup> did not align (Figure 9, Panel C), whereas SC cells at 10.0 dynes/cm<sup>2</sup> did (Figure 9, Panel D). Cell alignment in SC cells began after three to four days and by the end of one week there was full alignment.

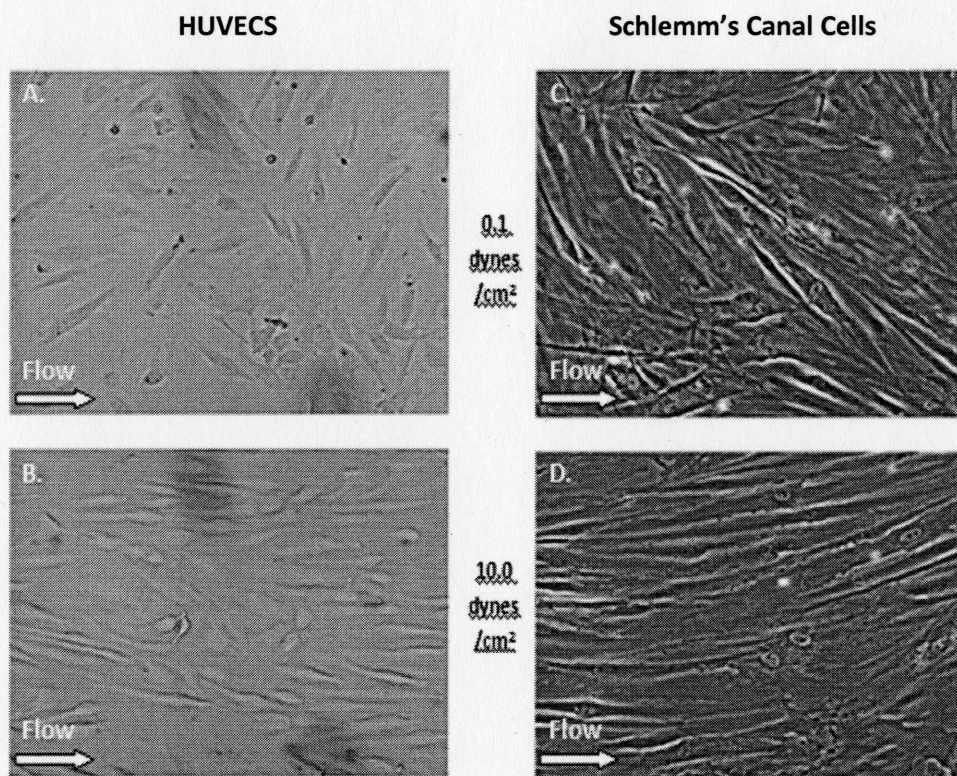


Figure 9: Cell Alignment in HUVECS (Panel A and B) and SC cells (Panel C and D) at 0.1 dynes/cm<sup>2</sup> and 10.0 dynes/cm<sup>2</sup>, respectively

## 4.1 Nitric Oxide Probe Analysis

### 4.1.0 Comparison of two NO detection Methods

The first step in using this NO probe was to determine which set-up was necessary for measuring the NO concentration with respect to shear stress being applied to HUVECs. The following calibration curve (Figure 10) was used in order to determine the NO concentration with respect to the shear.

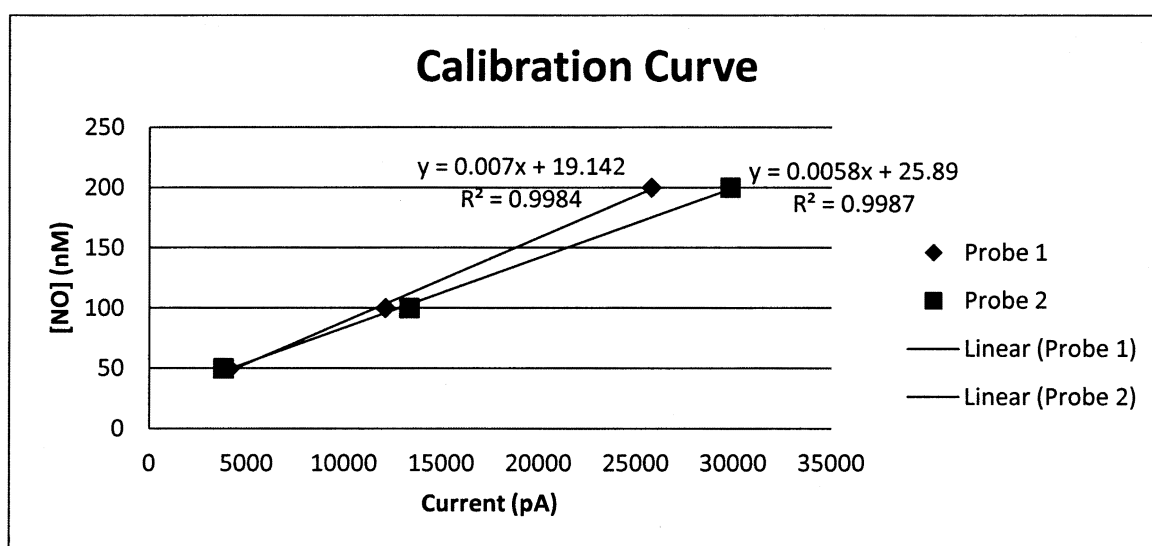


Figure 10: Calibration Curve for NO probe set-up 1 and 2. Probe 1 was used for the first set-up in which the NO probe was placed in the reservoir. Probe 2 was the NO probe used in the second set-up, in which the NO probe was connected to the system via a Y-connector.

The following five figures display the NO program of the experiment comparing the two potential NO probe set-ups for HUVECS set at 10.0 dynes/cm<sup>2</sup> for 24 hours. The first set-up is indicated by the blue line and, as can be seen, there is no noticeable change in NO production over the course of the experiment. The second set-up is indicated by the red line and shows an increase in current after approximately 70 minutes of being exposed to shear. This increase then levels at ~14,000 pA (107.09 nM NO) above the initial starting current. The NO production

decreases after several hours until it decreases to a current of  $\sim 6,000$  pA ( $60.69$  nM NO) above the initial starting current. As only the second set-up showed a response, it was the set-up that was used for the NO detection experiments.

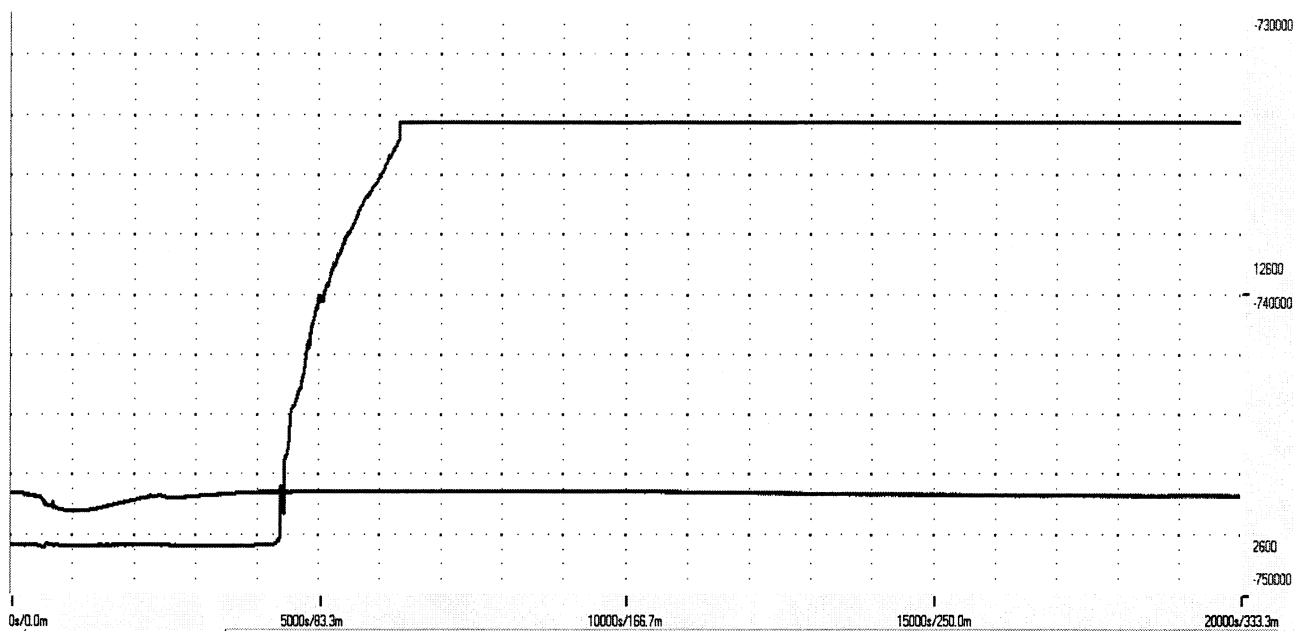


Figure 11: Comparing the response of the NO probe when probe is arranged in the First Set-Up (blue line) and in the Second Set-Up (red line). This figure shows the first 333 minutes of the experiment. The second set-up shows a relative increase in current around 70 minutes

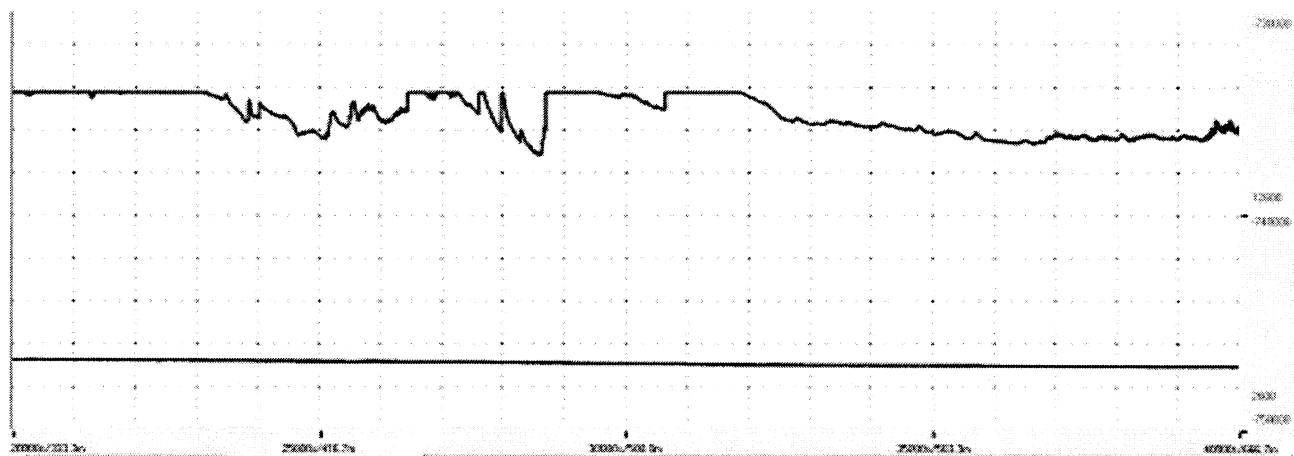


Figure 12: NO probe readings from 333 minutes to 666 minutes. The current is beginning to decrease.

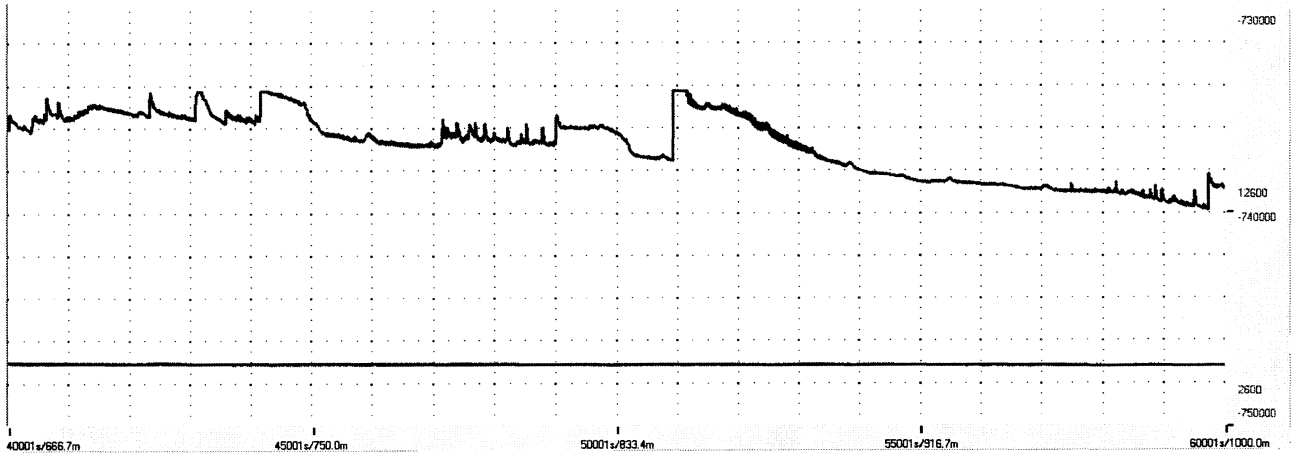


Figure 13: NO probe readings from 666 minutes to 1000 minutes

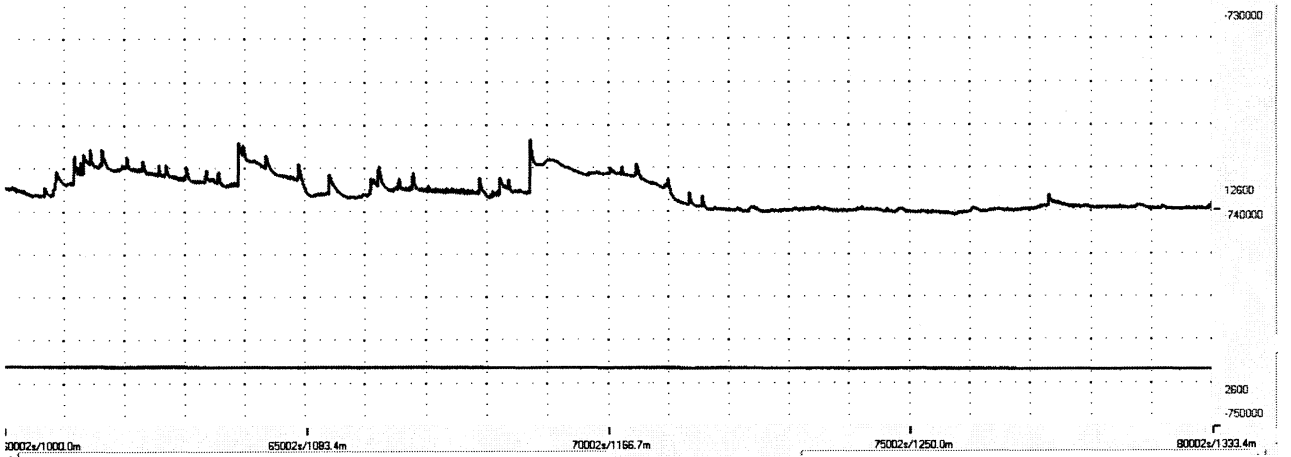


Figure 14: NO probe readings from 1000 minutes to 1333 minutes

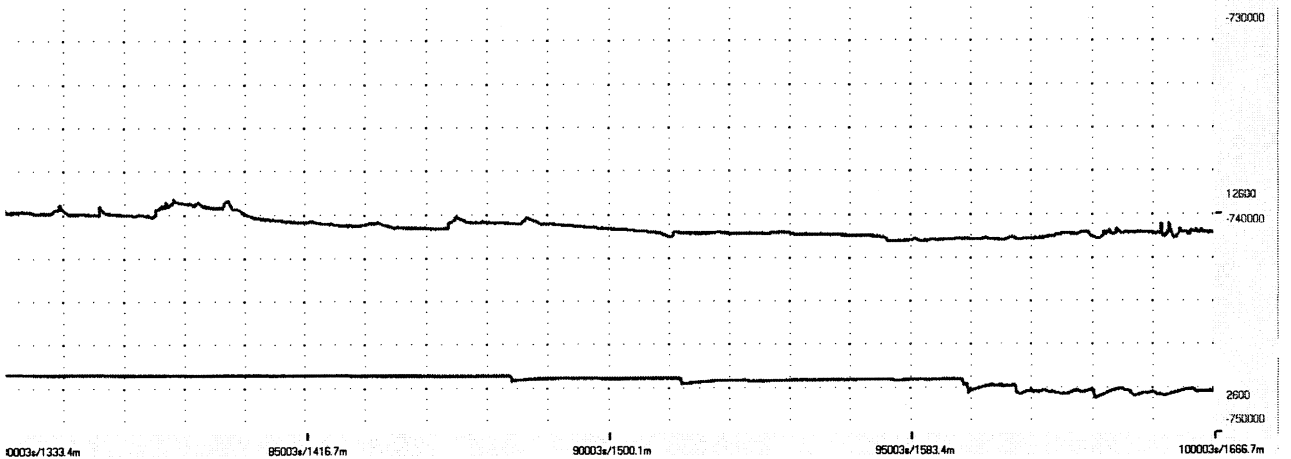


Figure 15: NO probe readings from 1333 minutes to 1666 minutes



Once it was decided that the second set-up with the Y-connector would be used, the same procedure for setting up the second set-up was used for the future experiments.

## **4.2 DAF-FM Fluorescence Analysis**

### **4.2.0 HUVECS and SC DAF-FM Figures**

The fluorescent images captured for each of the four conditions in HUVECS and SC cells. Cells exposed to  $0.1 \text{ dynes/cm}^2$  have less fluorescence than that of cells exposed to  $10.0 \text{ dynes/cm}^2$ . Exposure to L-Arginine conditions resulted in a noticeable increase in fluorescence while exposure to L-Name conditions resulted in a decrease in fluorescence in comparison to the L-Arginine conditions.

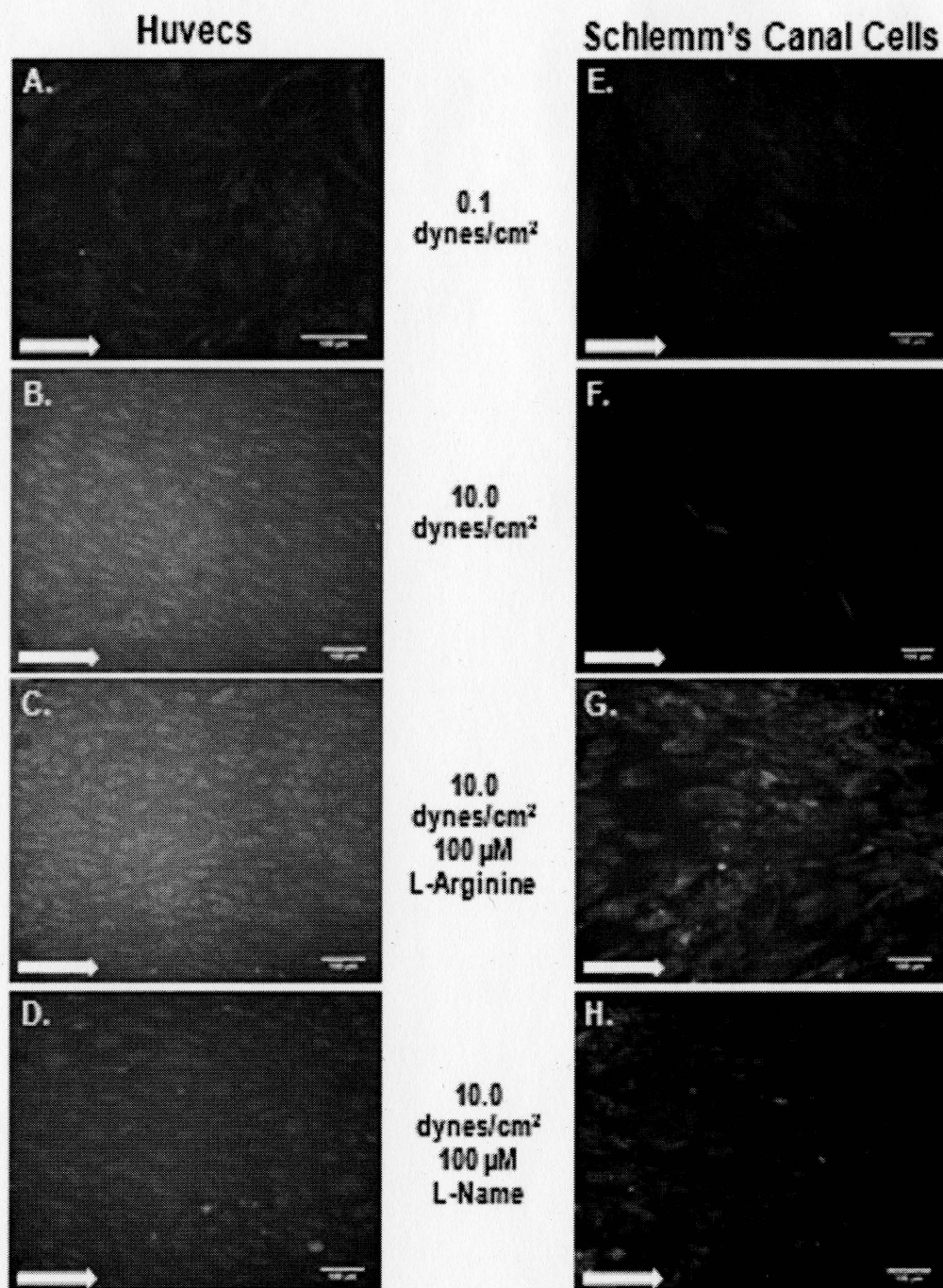


Figure 16: Nitric Oxide Production in HUVECS and Schlemm's Canal Cells. Panel A and E: 50  $\mu\text{M}$  DAF-FM probe treatment of Huvecs and Schlemm's Canal (SC) Cells, respectively, exposed to 0.1 dynes/cm<sup>2</sup> shear. Huvecs were exposed for 24 hours and SC cells were exposed for 1 week. *Panel B and F:* Huvecs and SC cells exposed to 10.0 dynes/cm<sup>2</sup>. *Panel C and G:* Positive Control – Huvecs and SC Cells exposed to 10.0 dynes/cm<sup>2</sup> with 100  $\mu\text{M}$  of NO Donor (L-Arginine) supplemented media. *Panel D and H:* Negative Control – Huvecs and SC Cells exposed to 10.0 dynes/cm<sup>2</sup> with 100  $\mu\text{M}$  eNOS inhibitor (L-Name) supplemented media.

#### 4.2.1 Quantification of NO Fluorescence

Image J software was used to quantify the average fluorescence across a  $\mu$ -slide after exposed to the four shear conditions. As shown in Figure 17, the increase in shear from 0.1 dynes/cm<sup>2</sup> to 10.0 dynes/cm<sup>2</sup> resulted in an increase in fluorescence from 41.8 to 106.5 in HUVECS and from 46.9 to 106.5 in SC. When the media was supplemented with L-Arginine, there is also a marked increase in fluorescence, particularly in the SC cell line. HUVECS treated with L-Name, resulted in fluorescence similar to that achieved by 0.1 dynes/cm<sup>2</sup>; however SC cells did not show this given the same media supplementation.

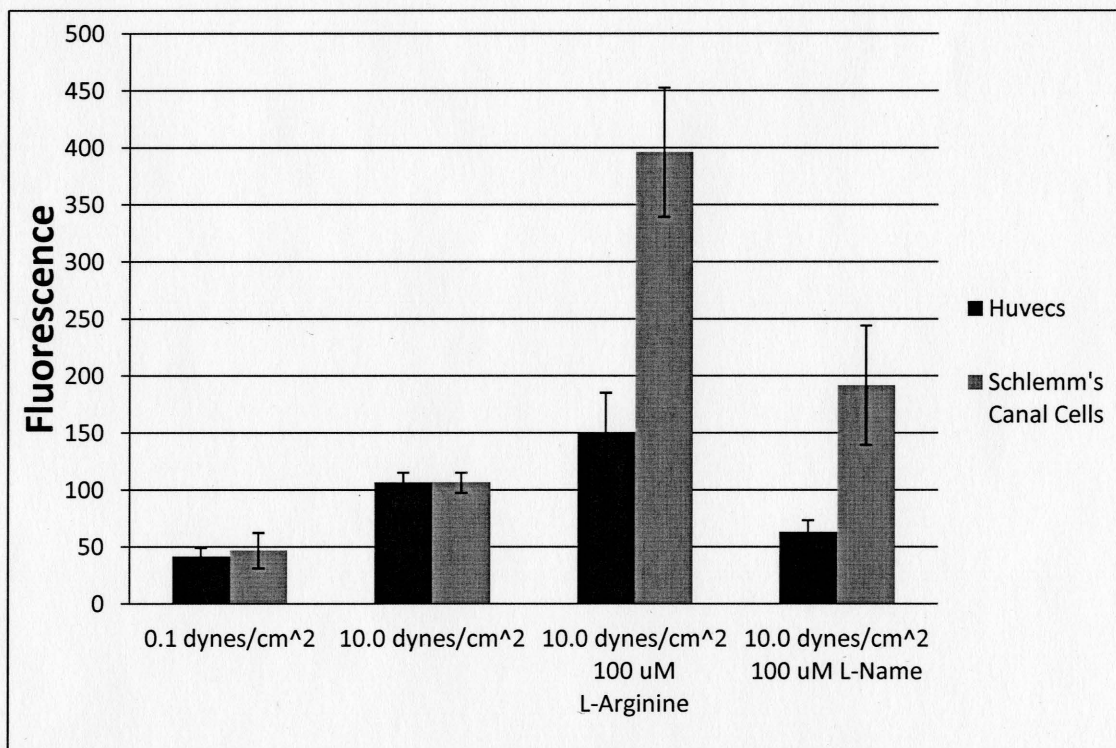


Figure 17: Relative Fluorescence of HUVECS and SC Cells exposed to different conditions (n=5).

## 5 DISCUSSION

With respect to cell alignment, SC cells behaved similarly to HUVECs in that the cells aligned with the applied shear flow. Likewise, SC cells produced more NO with an increase in shear flow.

### 5.0 Cell Alignment

For both HUVECS and SC cells, exposure to shear with the Ibidi Pump System resulted in cells aligning in parallel with the direction flow as predicted. For HUVECS, full alignment across the cell took 24 hours. For SC cells, full alignment took at least one week. Previous experiments support this cell alignment within HUVECS once exposed to relatively high shear stresses (12 and 15 dynes/cm<sup>2</sup>) for approximately 24 hours<sup>34,38</sup>. Likewise, Ethier, suggested a similar alignment as a result of shear stress in SC cells<sup>7</sup>, though no cell culture experiments have been performed on cultured SC cells. Further experimentation is needed in order to verify cell viability, such as through a propidium iodide dye. This will allow us to better control for the number of cells with respect to the NO production.

### 5.1 Expression of Nitric Oxide

#### 5.1.0 NO Probe

The Nitric Oxide Probe is capable of measuring relative concentration of NO across the cells at a given point in time. Generally, these probes are used to measure the NO concentrations in static cultured cells. As shown in Figure 11-Figure 15, it was found that the second set-up was necessary in order to have any noticeable NO readings. The current, and consequently the NO concentration, is shown to increase around 70 minutes; around 10 minutes or so after the HUVECS were beginning to be exposed to the 10.0 dynes/cm<sup>2</sup> of shear.

This second set-up is necessary potentially because NO degrades to nitrite within seconds<sup>39</sup>. When NO is exposed to superoxide, it degrades at a rate of  $6.7 \times 10^9 \text{ M}^{-1}/\text{s}^{-1}$ <sup>19</sup>. Because of this degradation rate, it is possible that the NO degraded in the media before the nitric oxide could reach the sensor in the reservoir. The NO would have had to travel through the tubes which have a length of 50 cm (Table 1) for the first set-up in comparison to a distance of approximately 2 cm in the second set-up.

Once selecting the second set-up, with the NO probe being placed in the Y-connector, however, other problems arose. The main problem that arose was the sensitivity of the permeable membrane that covers the sensor. When exposed to the shear the membrane gradually degraded or cracked leading to a loss in sensor sensitivity. With this loss in sensitivity, the sensor began reading very large and very steady current (~360,000 pA) which would take a long time to decrease, if the reading decreased at all, even with being removed from the media. Working probes respond to every movement of the probe (Figure 18). The company was contacted to assist in making the membrane more robust, however even this new probe came to the same result though this sensor did take longer before it to become unresponsive to changes in the NO current.

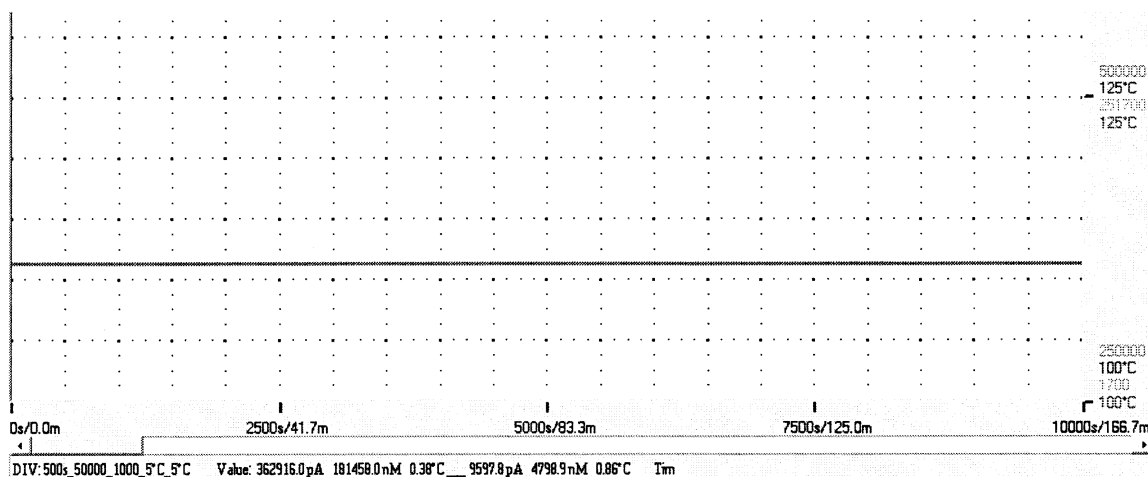


Figure 18: Desensitized NO probe reading at ~360,000 pA

It is possible to connect the probe to a side tube of some sort and only have the probe take measurements at selected intervals; however, this probe responds to movement and takes several hours to stabilize to the media. This makes it difficult to distinguish between the responses to the movement of the probe versus the responses to the Nitric Oxide in the solution.

Though the probe would generally work for the first experiments (as shown in Figure 12) and show an increase in the NO concentration, by the second or even third experiment, the probe would be desensitized. Consequently, use of this NO probe was not the most efficient method for measuring NO.

### 5.1.1 DAF-FM Diacetate Fluorescence

The DAF-FM Diacetate Fluorescence probe is a molecular probe that is capable of crossing through the cell membrane. Upon incubation with this probe, cells fluoresce indicating a relative amount of Nitric Oxide in the cells.

Figure 17 shows that an increase in shear from 0.1 to 10.0 dynes/cm<sup>2</sup> does result in an increase in the fluorescence in both cell types. An increase in fluorescence is also seen when a NO donor is added to the media, as expected of a positive control. A result similar to 0.1 dynes/cm<sup>2</sup> was achieved when adding an eNOS inhibitor to the media in HUVECS though not in SC. In fact, the fluorescence was larger than even the fluorescence achieved in 10.0 dynes/cm<sup>2</sup>. A potential reason for this is that the L-Name eNOS inhibitor degraded over the course of the week, resulting in NO being expressed despite the original media conditions. It is possible that the NO was being produced by another Nitric Oxide synthase.

Typically, the media is not replaced during the week in which SC are exposed to shear due to contamination issues, however because of this result, it may be necessary to replace the media with fresh media supplemented with L-Name.

Other studies have also indicated that a shear stress dose dependently up-regulates NO synthesis in cultured endothelial cells<sup>40, 41</sup>. This supports the DAF-FM fluorescence data received for HUVECS, in that an increase in shear resulted in an increase in fluorescence. In these experiments, however, NO was measured indirectly by measuring [<sup>3</sup>H] L-Citrulline formation<sup>40</sup> or cGMP production<sup>41</sup>. cGMP synthesis is stimulated by NO activating guanylate cyclase which is the enzyme that catalyzes cGMP synthesis. Therefore, we can only indirectly compare the amount of NO that was produced.

## 6 FUTURE WORK

There are several more future experiments that are recommended in order to understand the effects that shear has on Schlemm's Canal.

First of all, more HUVEC experiments are required at the four conditions given in this work in order to determine statistical significance in more than one  $\mu$ -slide per condition. This is particularly the case with the NO donor and the eNOS inhibitor conditions as preliminary experiments showed that no eNOS protein appeared in Western Blots, potentially due to there being too few cells on the  $\mu$ -slides.

It is possible that dose response curves comparing the concentration of L-Arginine or L-Name will be necessary in order to determine a concentration that will result in production of the enzyme eNOS. Or else, another method, besides Western Blot may be needed in order to detect eNOS. Another NOS inhibitor, for nNOS or iNOS, will also help us determine if eNOS is the enzyme responsible for maintaining the nitric oxide production in SC cells.

Because the DAF-FM fluorescence is taken at different time points, the HUVECS at 24 hours and the SC at 1 week, it is difficult to directly compare the two cell types with respect to DAF-FM fluorescence. Therefore, applying the DAF-FM to the HUVECS and the SC at similar time points over the course of the week would allow us to more directly compare the two cell types, rather than comparing the two when the cells reach full cell alignment.

Another method of detecting the amount of Nitric Oxide, as a secondary measure to the DAF-FM Fluorescent probe would also help to confirm the results we have been receiving. Ideally this detection method will be a more direct measurement of NO. A potential method to explore



would be to use an assay to quantify the amount of nitrite (which is what NO is degraded to), with respect to the amount of media, at the various shears stresses.

To improve the cells ability to remain attached to the  $\mu$ -slide, other treatments on the  $\mu$ -slide could be tried. This may also assist in speeding up the amount of time that SC cells need to incubate before shear can be applied. Regardless, other shear stresses are also going to be performed to better determine the range of NO production and eNOS expression with respect to shear. Potential shear stresses include 1.0, 5.0 and 15.0 dynes/cm<sup>2</sup>.

With this system now functional, there are a variety of other proteins besides eNOS that can be measured: VE-cadherin, Endothelin-1 and actin. VE-cadherin is a glycoprotein that mediates cell-cell adhesion and is calcium-dependent<sup>42</sup>. It has come to be an indicator of endothelial cells. Endothelin-1 (ET-1) is another important modulator of vascular tone in the human ophthalmic artery is the vasoconstrictor<sup>43</sup>. ET-1 produces the vasoconstriction of the anterior optic nerve vasculature and thus may contribute to the regulation of IOP and vessel tone<sup>27,44</sup>. Actin, is a cytoskeletal protein that assists in maintaining the structure of the cell. Staining for actin will allow us to confirm that the cells are aligned with each other. Another method for analyzing cell alignment would be through the use of light microscopy.

It is unclear whether low shear stress or oscillatory shear stress is more important for the expression of eNOS<sup>30</sup>. With the use of the Ibidi Pump system, future experiments can explore the option of exposing cells to pulsatile shear flow and determine if there is a difference between oscillatory and continuous shear flow on cells. Therefore, with the use of a second fluidic unit, we can test the effects of pulsatile flow on both HUVECS and SC cells.

Once the HUVECS are fully tested for these proteins, etc., further normal human SC primary cell lines (two to three cell lines) would also be required to adequately compare the HUVEC results to the SC. Particular focus will need to be paid to the shear condition in which the media is supplemented with eNOS inhibitor as the DAF-FM fluorescence was higher than even the 10.0 dynes/cm<sup>2</sup> results. Once normal SC cells are fully characterized, they can be compared to glaucomatous SC cells lines.

As Trabecular Meshwork cells are also a part of the conventional outflow pathway and are also known for producing NO, it would also be interesting to see what the effect of shear has on TM cells. Experiments have shown that, at the cellular level, Nitric Oxide relaxes TM cells and result in decreases in cell volume and increased in outflow facility<sup>45</sup>.

The increase in NO production in SC cells with an increase in shear suggests that shear in Schlemm's Canal, likewise, promotes the production of NO. With these suggested future experiments, we will be able to better determine if NO production is an important IOP regulatory factor that is somehow impaired in glaucoma patients.

## **7 CONCLUSIONS**

Human Schlemm's Canal cells respond to shear stress similarly to other vascular endothelial cells. When exposed to shear, SC cells align with flow over the course of a week and preliminary experiments have shown that an increase in shear, results in an increase in NO production as shown by a DAF-FM fluorescent probe. Further experiments are needed to determine if this applies to further cell lines and if a similar effect can be seen in the SC cell's expression of eNOS.

## APPENDIX

### Shear Stress on Schlemm's Canal <sup>7</sup>

Shear stress on Schlemm's Canal was derived by Ethier's group <sup>7</sup> by treating Schlemm's Canal as having an elliptical cross section with a major and minor axes of  $a$  and  $b$ . It is assumed that this cross section is uniform and the wall is porous, allowing aqueous humor to seep in. The porous nature of this model also allows for the collector channels to be factored into the model. The flow rate in the SC,  $Q(x)$ , is then defined by:

$$\frac{dQ}{dx} = \frac{IOP - p(x)}{R_{iw}} \quad (\text{Equation 2})$$

Where  $p(x)$  is the local pressure within the SC,  $IOP$  is intraocular pressure (this value is assumed to be constant), and  $1/R_{iw}$  is the hydraulic conductivity of the trabecular meshwork and inner wall of the SC, per a unit length of the inner wall (this value is also assumed to be constant). The  $x$  is set to 0 at the midway point between two collector channels and  $x$  is set to  $\pm L$  for the location of the nearest collector channel.

Pressure is related to shear stress by:

$$\frac{dp}{dx} = \frac{\tau_w(x)C}{A} \quad (\text{Equation 3})$$

Where  $\tau_w$  is the wall shear stress,  $A$  is the cross sectional area of the SC and  $C$  is the perimeter of the cross section.

The velocity profile is given by:

$$u = \frac{2Q(x)}{A} \left[ 1 - \frac{y^2}{b^2} - \frac{z^2}{a^2} \right] \quad (\text{Equation 4})$$

With the major axis,  $a$ , being along the  $y$ -direction; and minor axis,  $b$ , being along the  $z$ -direction. The wall shear stress,  $\tau_w$ , varies with its position and its mean value is:

$$\overline{\tau_w}(x) = \frac{\mu Q(x)(1+(a/b)^2)}{ab^2 E(1-(a/b)^2)} \quad (\text{Equation 5})$$

Here,  $E$  is the elliptical integral of the second kind. Minimum and maximum shear stresses are given by:

$$\tau_{w,min} = \frac{4\mu Q(x)}{\pi a^2 b} \quad (\text{Equation 6})$$

$$\tau_{w,max} = \frac{4\mu Q(x)}{\pi a b^2} \quad (\text{Equation 7})$$

With the boundary conditions of  $Q(x)=0$  at  $x=0$  and  $Q(x)=Q_{total}/(2N)$  at  $x=\pm L$  ( $Q_{total}$  is the total flow rate that enters the canal and  $N$  is the number of collector channels) we get:

$$Q(x) = \frac{Q_{total}}{2N} \frac{\sinh(kx)}{\sinh(kL)} \quad (\text{Equation 8})$$

With

$$k^2 = \frac{4\mu(1+(a/b)^2)}{\pi a b^3 R_{iw}} \quad (\text{Equation 9})$$

## Ibidi Pump Shear Stress Calculations

Shear stresses were calibrated by observing the flow rate going through the system. The computer then used the Ibidi Pump System Program to calculate the shear with the following equation for the  $\mu$ -Slide I<sup>0.6</sup>:

$$\tau \left[ \frac{\text{dynes}}{\text{cm}^2} \right] = 5.129\Phi \left[ \frac{\text{ml}}{\text{min}} \right] \quad (\text{Equation 10})$$

Where  $\tau$  is the shear stress and  $\phi$  is the flow rate.

This equation was derived in an application note provided by the Ibidi Company<sup>46</sup>. The local flow velocity,  $v(x,y)$  was originally calculated by Cornish<sup>47</sup>. The  $\mu$ -slide channel was treated as a rectangular cross-section through which flow passes:

$$v(x, y) = -\frac{1}{\eta} \frac{dp}{dz} \left\{ \frac{b^2}{2} - \frac{x^2}{2} - \sum_{n=0}^{\infty} \frac{(-1)^n (2b^2)}{(2n+1)^3} \left( \frac{2}{\pi} \right)^3 \frac{\cosh \left[ (2n+1) \left( \frac{\pi y}{2b} \right) \right]}{\cosh \left[ (2n+1) \left( \frac{\pi h}{2b} \right) \right]} \cos \left[ \frac{(2n+1)\pi x}{2b} \right] \right\} \quad (\text{Equation 11})$$

The total flow,  $\phi$ , was calculated through the channel with:

$$\Phi = -\frac{1}{\eta} \frac{dp}{dz} \left( \frac{4}{3} hb^3 - 8b^4 \left( \frac{2}{\pi} \right)^5 \sum_{n=0}^{\infty} \frac{1}{(2n+1)^5} \tanh \left[ \frac{(2n+1)\pi h}{2b} \right] \right) \quad (\text{Equation 12})$$

Where  $2h$  is the height of the channel in the  $y$ -axis direction,  $2b$  is the width of the channel in the  $x$ -direction and the  $z$ -axis is the direction of the flow (Figure 19). The change in pressure along the channel is denoted by  $dp/dz$ .

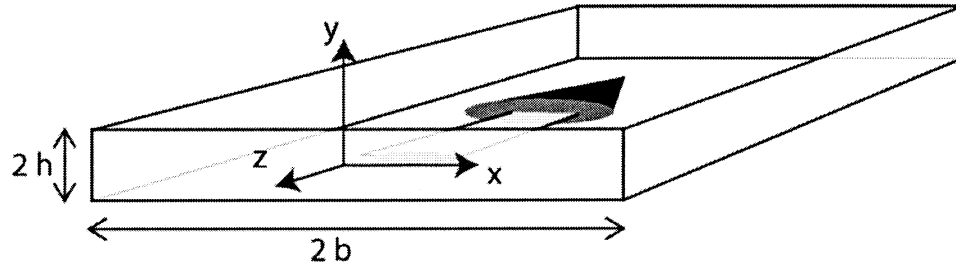


Figure 19: Schematic of Flow through a Rectangular Cross Section <sup>46</sup>

The change in pressure is eliminated with setting:

$$q = \left( \frac{4}{3} hb^3 - 8b^4 \left( \frac{2}{\pi} \right)^5 \sum_{n=0}^{\infty} \frac{1}{(2n+1)^5} \tanh \left[ \frac{(2n+1)\pi h}{2b} \right] \right) \quad (\text{Equation 13})$$

Therefore

$$\frac{dp}{dz} = -\eta \frac{\Phi}{q} \quad (\text{Equation 14})$$

Shear stress is then calculated by setting  $y = -h$ .

$$\tau(x, y) = \eta \frac{\partial v(x, y)}{\partial y} = -\eta \frac{1}{\eta} \frac{dp}{dz} \left\{ \sum_{n=0}^{\infty} \frac{(-1)^n b \pi}{(2\pi+1)^2} \left( \frac{2}{\pi} \right)^3 \frac{\sinh \left[ (2n+1) \frac{(\pi y)}{2b} \right]}{\cosh \left[ (2n+1) \frac{(\pi h)}{2b} \right]} \cos \left[ \frac{(2n+1)\pi x}{2b} \right] \right\} \quad (\text{Equation 15})$$

Eliminating  $dp/dz$ :

$$\begin{aligned} \tau(x, y) &= -\eta \frac{1}{\eta} \left\{ \sum_{n=0}^{\infty} \frac{(-1)^n b \pi}{(2\pi+1)^2} \left( \frac{2}{\pi} \right)^3 \frac{\sinh \left[ (2n+1) \frac{(\pi y)}{2b} \right]}{\cosh \left[ (2n+1) \frac{(\pi h)}{2b} \right]} \cos \left[ \frac{(2n+1)\pi x}{2b} \right] \right\} = \\ &\eta \frac{\Phi}{q} \left\{ \sum_{n=0}^{\infty} \frac{(-1)^n b \pi}{(2\pi+1)^2} \left( \frac{2}{\pi} \right)^3 \frac{\sinh \left[ (2n+1) \frac{(\pi y)}{2b} \right]}{\cosh \left[ (2n+1) \frac{(\pi h)}{2b} \right]} \cos \left[ \frac{(2n+1)\pi x}{2b} \right] \right\} \quad (\text{Equation 16}) \end{aligned}$$

As cells typically attach to the bottom of the  $\mu$ -slide channel:

$$\tau(x = 0, y = -h) = \eta \frac{\Phi}{q} \left\{ \sum_{n=0}^{\infty} \frac{(-1)^n b \pi}{(2\pi+1)^2} \left( \frac{2}{\pi} \right)^3 \tanh \left[ \frac{(2n+1)\pi h}{2b} \right] \right\} \quad (\text{Equation 17})$$

## References

1. Glaucoma Research Foundation. Glaucoma facts and stats. March 23, 2012;2012.
2. Glaucoma Research Foundation. Types of glaucoma. May 24, 2011;2012.
3. Lei Y, Overby DR, Boussoimmier-Calleja A, Stamer WD, Ethier CR. Outflow physiology of the mouse eye: Pressure dependence and washout. *Invest.Ophthalmol.Vis.Sci.* 2011;52:1865-71.
4. Borghi V., Bastia E., Guzzetta M., et al. A novel nitric oxide releasing prostaglandin analog, NCX 125, reduces intraocular pressure in rabbit, dog, and primate models of glaucoma. *J.Ocul.Pharmacol.Ther.Journal of Ocular Pharmacology and Therapeutics* 2010;26:125-131.
5. [Anonymous]. The advanced glaucoma intervention study (AGIS): 7. the relationship between control of intraocular pressure and visual field deterioration. *Am.J.Ophthalmol.* 2000;130:429-440.
6. Mäepea O, Bill A. The pressures in the episcleral veins, schlemm's canal and the trabecular meshwork in monkeys: Effects of changes in intraocular pressure. *Exp.Eye Res.* 1989;49:645-63.
7. Ethier CR, Read AT, Chan D. Biomechanics of schlemm's canal endothelial cells: Influence on F-actin architecture. *Biophys.J.* 2004;87:2828-37.
8. Stamer WD, Lei Y, Boussoimmier-Calleja A, Overby DR, Ethier CR. eNOS, a pressure-dependent regulator of intraocular pressure. *Invest.Ophthalmol.Vis.Sci.* 2011;52:9438-44.
9. Mäepea O, Bill A. Pressures in the juxtacanalicular tissue and schlemm's canal in monkeys. *Exp.Eye Res.* 1992;54:879-83.
10. Krohn J. Expression of factor VIII-related antigen in human aqueous drainage channels. *Acta Ophthalmol.Scand.* 1999;77:9-12.
11. Hamanaka T, Bill A, Ichinohasama R, Ishida T. Aspects of the development of schlemm's canal. *Exp.Eye Res.* 1992;55:479-88.
12. Doriot PA, Dorsaz PA, Dorsaz L, De Benedetti E, Chatelain P, Delafontaine P. In-vivo measurements of wall shear stress in human coronary arteries. *Coron.Artery Dis.* 2000;11:495-502.
13. Michel T, Feron O. Nitric oxide synthases: Which, where, how, and why? *The Journal of Clinical Investigation.* 1997;100:2146.



14. Bryan N, S. Discovery of the nitric oxide signaling pathway and targets for drug development. *Front Biosci Frontiers in Bioscience* 2009.
15. Colasanti M, Suzuki H. The dual personality of NO. *Trends Pharmacol.Sci.* 2000;21:249-52.
16. Becquet, F., Courtois, Y., & Goureau, O. Nitric oxide in the eye: Multifaceted roles and diverse outcomes. *Survey of Ophthalmology* January 01, 1997;42:71-82.
17. Moncada S, Palmer RM, Higgs EA. Nitric oxide: Physiology, pathophysiology, and pharmacology. *Pharmacol.Rev.* 1991;43:109-42.
18. Predescu D, Predescu S, Shimizu J, Miyawaki-Shimizu K, Malik AB. Constitutive eNOS-derived nitric oxide is a determinant of endothelial junctional integrity. *American Journal of Physiology.Lung Cellular and Molecular Physiology* 2005;289:371-81.
19. Harrison DG. Cellular and molecular mechanisms of endothelial cell dysfunction. *The Journal of Clinical Investigation.* 1997;100:2153.
20. Kotikoski, H., Vapaatalo, H., & Oksala, O. Nitric oxide and cyclic GMP enhance aqueous humor outflow facility in rabbits. *Current Eye Research* January 01, 2003;26:119-123.
21. Polak K, Luksch A, Berisha F, Fuchsjaeger-Mayrl G, Dallinger S, Schmetterer L. Altered nitric oxide system in patients with open-angle glaucoma. *Arch.Ophthalmol.* 2007;125:494-8.
22. Schneemann A, Dijkstra BG, van den Berg TJ, Kamphuis W, Hoyng PF. Nitric oxide/guanylate cyclase pathways and flow in anterior segment perfusion. *Graefe's Archive for Clinical and Experimental Ophthalmology = Albrecht Von Graefes Archiv Für Klinische Und Experimentelle Ophthalmologie* 2002;240:936-41.
23. Nathanson JA. Nitric oxide and nitrovasodilators in the eye: Implications for ocular physiology and glaucoma. *J.Glaucoma* 1993;2:206-10.
24. Nathanson JA, McKee M. Alterations of ocular nitric oxide synthase in human glaucoma. *Invest.Ophthalmol.Vis.Sci.* 1995;36:1774-84.
25. Schuman J, Erickson K, Nathanson J. Nitrovasodilator effects on intraocular pressure and outflow facility in monkeys. *Exp.Eye Res.* 1994;58:99-105.
26. Nathanson JA, McKee M. Identification of an extensive system of nitric oxide-producing cells in the ciliary muscle and outflow pathway of the human eye. *Invest.Ophthalmol.Vis.Sci.* 1995;36:1765-73.
27. Tunny TJ, Richardson KA, Clark CV. Association study of the 5' flanking regions of endothelial-nitric oxide synthase and endothelin-1 genes in familial primary open-angle glaucoma. *Clin.Exp.Pharmacol.Physiol.* 1998;25:26-9.

28. Yamamoto R, Bredt DS, Snyder SH, Stone RA. The localization of nitric oxide synthase in the rat eye and related cranial ganglia. *Neuroscience* 1993;54:189-200.
29. Harrison DG, Sayegh H, Ohara Y, Inoue N, Venema RC. Regulation of expression of the endothelial cell nitric oxide synthase. *Clin.Exp.Pharmacol.Physiol.* 1996;23:251-5.
30. Cheng C, van Haperen R, de Waard M, et al. Shear stress affects the intracellular distribution of eNOS: Direct demonstration by a novel in vivo technique. *Blood* 2005;106:3691-8.
31. Ziegler T, Silacci P, Harrison VJ, Hayoz D. Nitric oxide synthase expression in endothelial cells exposed to mechanical forces. *Hypertension* 1998;32:351-5.
32. Ibidi. Ibidi - cells in focus: FAQ. 2010;2012:1.
33. Ibidi. Ibidi pump instruction manual version 1.5.0. November 3, 2011;2011:53.
34. Ibidi. Application note 13: Flow experiment with the ibidi pump system and u-slide I<sup>0.6</sup> luer. March 18, 2011;2012:8.
35. Molecular Probes I. Nitric oxide indicators: DAF-FM and DAF-FM diacetate. May 16, 2001;2012:3.
36. Sumida G.M., Stamer W.D. S1P<sub>2</sub> receptor regulation of sphingosine-1-phosphate effects on conventional outflow physiology. *Am.J.Physiol.Cell Physiol.American Journal of Physiology - Cell Physiology* 2011;300:C1164-C1171.
37. Sumida G.M., Daniel Stamer W. Sphingosine-1-phosphate enhancement of cortical actomyosin organization in cultured human schlemm's canal endothelial cell monolayers. *Invest.Ophthalmol.Vis.Sci.Investigative Ophthalmology and Visual Science* 2010;51:6633-6638.
38. Albuquerque ML, Waters CM, Savla U, Schnaper HW, Flozak AS. Shear stress enhances human endothelial cell wound closure in vitro. *American Journal of Physiology.* 2000;279:H293-H302.
39. Hakim TS, Sugimori K, Camporesi EM, Anderson G. Half-life of nitric oxide in aqueous solutions with and without haemoglobin. *Physiol.Meas.* 1996;17:267-77.
40. Noris M, Morigi M, Donadelli R, et al. Nitric oxide synthesis by cultured endothelial cells is modulated by flow conditions. *Circ.Res.* 1995;76:536-43.
41. Knudsen HL, Frangos JA. Role of cytoskeleton in shear stress-induced endothelial nitric oxide production. *Am.J.Physiol.* 1997;273:347-55.

42. Heimark R, Kaochar S, Stamer W. Human schlemm's canal cells express the endothelial adherens proteins, VE-cadherin and PECAM-1. *Curr.Eye Res.* 2002;25:299-308.
43. Haefliger IO, Flammer J, Lüscher TF. Nitric oxide and endothelin-1 are important regulators of human ophthalmic artery. *Invest.Ophthalmol.Vis.Sci.* 1992;33:2340-3.
44. MacCumber MW, Jampel HD, Snyder SH. Ocular effects of the endothelins. abundant peptides in the eye. *Arch.Ophthalmol.* 1991;109:705-9.
45. Dismuke WM, Mbadugha CC, Ellis DZ. NO-induced regulation of human trabecular meshwork cell volume and aqueous humor outflow facility involve the BKCa ion channel. *American Journal of Physiology.Cell Physiology.* 2008;63:C1378.
46. Ibbi. Application note 11: Shear stress and shear rates for all channel  $\mu$ -slides - based on numerical calculation. October 27, 2010;2012:18.
47. Cornish RJ. Flow in a pipe of rectangular cross-section. *Proceedings of the Royal Society of London.Series A, Containing Papers of a Mathematical and Physical Character* 1928;120:691-700.